EUROPEAN ORGANIZATION FOR NUCLEAR RESEARCH

CERN-EP/86-99
29 July 1986

# $\rho^0$ and $\omega$ PRODUCTION IN DEEP INELASTIC $\mu$-p INTERACTIONS AT 280 GeV/c

The European Muon Collaboration

Aachen[1], CERN[2], DESY (Hamburg)[3], Freiburg[4], Hamburg (University)[5], Kiel[6], LAL (Orsay)[7], Lancaster[8], LAPP (Annecy)[9], Liverpool[10], Marseille[11], Mons[12], MPI (München)[13], Oxford[14], RAL (Chilton)[15], Sheffield[16], Torino[17], Uppsala[18], Warsaw[19], Wuppertal[20].

M. Arneodo[17], A. Arvidson[18], J.J. Aubert[11], B. Badelek[19a)], J. Beaufays[2], C.P. Bee[8b)], C. Benchouk[11], G. Berghoff[1], I. Bird[8c)], D. Blum[7], E. Böhm[6], X. de Bouard[9], F.W. Brasse[3], H. Braun[20], C. Broll[9+)], S. Brown[10d)], H. Brück[20e)], H. Calen[18], J.S. Chima[15f)], J. Ciborowski[19a], R. Clifft[15], G. Coignet[9], F. Combley[16], J. Coughlan[8g)], G. D'Agostini[11], S. Dahlgren[18], F. Dengler[13], I. Derado[13], T. Dreyer[4], J. Drees[20], M. Düren[1], V. Eckardt[13], A. Edwards[20h)], M. Edwards[15], T. Ernst[4], G. Eszes[9i)], J. Favier[9], M.I. Ferrero[17], J. Figiel[5j)], W. Flauger[3], J. Foster[16k)], E. Gabathuler[10], J. Gajewski[5], R. Gamet[10], J. Gayler[3], N. Geddes[14l)], P. Grafström[18], F. Grard[12], J. Haas[4], E. Hagberg[18], F.J. Hasert[1m)], P. Hayman[10], P. Heusse[7], M. Jaffré[7], A. Jacholkowska[2], F. Janata[5], G. Jancso[9n)], A.S. Johnson[14o)], E.M. Kabuss[4], G. Kellner[2], V. Korbel[3], J. Krüger[20e)], S. Kullander[18], U. Landgraf[4], D. Lanske[1], J. Loken[14], K. Long[14p)], M. Maire[9], P. Malecki[13], A. Manz[13], S. Maselli[17n)], W. Mohr[4], F. Montanet[11], H.E. Montgomery[2q)], E. Nagy[9i)], J. Nassalski[19r)], P.R. Norton[15], F.G. Oakham[15s)], A.M. Osborne[2], C. Pascaud[7], B. Pawlik[13], P. Payre[11], C. Peroni[17], H. Peschel[20], H. Pessard[9], J. Pettingale[10], B. Pietrzyk[11], U. Pietrzyk[20], B. Pönsgen[5], M. Pötsch[20], P. Renton[14], P. Ribarics[9i)], K. Rith[4c)], E. Rondio[19a)], A. Sandacz[19r)], M. Scheer[1], A. Schlagböhmer[4], H. Schiemann[5], N. Schmitz[13], M. Schneegans[9], M. Scholz[1], T. Schröder[4], M. Schouten[13], K. Schultze[1], T. Sloan[8], H.E. Stier[4], M. Studt[5], G.N. Taylor[14], J.M. Thénard[9], J.C. Thompson[15], A. de la Torre[5t)], J. Toth[9i)], L. Urban[1], L. Urban[9i)], W. Wallucks[4], M. Whalley[16u)], S. Wheeler[16], W.S.C. Williams[14], S.J. Wimpenny[10p)], R. Windmolders[12], G. Wolf[13].

(Submitted to Zeitschrift für Physik C)

---

Abstract

Inclusive distributions of $\rho^0$ and $\omega$ mesons have been measured in deep inelastic $\mu$-p interactions at 280 GeV/c. A comparison of the $\rho^0$ cross sections with other leptoproduction experiments is presented. The $\omega$ results represent the first observation of this inclusive channel in high energy leptoproduction. The $\rho^0$ and $\omega$ yields are found to be equal as may be expected from the available density of states in isospin space. This contrasts with spin angular momentum where the vector to pseudoscalar meson ratio is suppressed relative to the available number of spin states.

---

For footnotes see next page

Addresses

1) III. Physikalisches Inst. A, Physikzentrum, Aachen, Germany.
2) CERN, Geneva, Switzerland.
3) DESY, Hamburg, Germany.
4) Fakultät für Physik, Universität Freiburg, Germany.
5) II Institut für Experimentalphysik, Universität Hamburg, Germany.
6) II Institut für Kernphysik, Universität Kiel, Germany.
7) Laboratoire de l'Accélérateur Linéaire, Université de Paris-Sud, Orsay, France.
8) Department of Physics, University of Lancaster, England.
9) Laboratoire d'Annecy de Physique des Particles, IN2P3, Annecy-le-Vieux, France.
10) Department of Physics, University of Liverpool, England.
11) Centre de Physique des Particules, Faculté des Sciences de Luminy, Marseille, France.
12) Faculté des Sciences, Université de L'Etat à Mons, Belgium.
13) Max-Planck-Institut für Physik und Astrophysik, München, Germany.
14) Nuclear Physics Laboratory, University of Oxford, England.
15) Rutherford and Appleton Laboratory, Chilton, Didcot, England.
16) Department of Physics, University of Sheffield, England.
17) Istituto di Fisica, Università di Torino, Italy.
18) Gustav Werners Institut, University of Uppsala, Sweden.
19) Physics Institute, University of Warsaw, and Institute for Nuclear Studies, Warsaw, Poland.
20) Fachbereich Physik, Universität Wuppertal, Germany.

a) University of Warsaw, Poland.
b) Now at University of Liverpool, England.
c) Now at MPI für Kernphysik, Heidelberg, Germany.
d) Now at TESA S.A., Renens, Switzerland.
e) Now at DESY, Hamburg, W. Germany.
f) Now at 30 Addison Ave., Hounslow, England.
g) Now at RAL, Chilton, Didcot, England.
h) Now at Jet, Joint Undertaking, Abingdon, England.
i) Now at Central Research Institute for Physics of the Hungarian Academy of Science, Budapest, Hungary.
j) Now at Institute of Nuclear Physics, Krakow, Poland.
k) Now at University of Manchester, England.
l) Now at British Telecom, London, England.
m) Now at Krupp Atlas Elektronic GmbH, Bremen, Germany.
n) Now at MPI, Munich, Germany.
o) Now at SLAC, Stanford, California.
p) Now at CERN, Geneva, Switzerland.
q) Now at FNAL, Batavia, Illinois, U.S.A.
r) Institute for Nuclear Studies, Warsaw, Poland.
s) Now at NCR, Ottawa, Canada.
t) Now at Universidad Nacional, Mar del Plata, Argentina.
u) Now at University of Durham, England.
+) Deceased

## 1. Introduction

Studies of inclusive vector meson leptoproduction have helped to increase present understanding of the quark fragmentation process. A large proportion of vector mesons are primary particles formed in the initial fragmentation chain. In contrast, pseudoscalar mesons are often the decay products of more massive resonances, particularly in the central region. Hence a study of vector mesons should give a greater insight into the hadronisation process.

The leptoproduction of hadrons can be described in terms of several models based on the quark-parton formalism. These models, however, all contain free parameters which can only be reliably determined from experiment. The vector to pseudoscalar meson production ratio is an example of such a parameter. One assumption of the Field-Feynman model [1] is that vector and pseudoscalar mesons are produced in the ratio 3:1 in accordance to the statistical population of their spin states. However, experiments which have studied the leptoproduction of $\rho^{o}$ mesons have not observed such high production rates [2-10]. In the Lund model [11] the vector to pseudoscalar meson ratio is set 1:1 (for the lowest mass mesons) in accordance with the measured value. It has been suggested that the suppression of vector mesons is due to the mass difference between pseudoscalar and vector mesons [12]. It is therefore of interest to compare the production of isovector and isoscalar mesons of equal masses, e.g. $\rho^{o}$ and $\omega$ to see if an analogous suppression occurs.

In the present paper results on inclusive $\rho^{o}$ and $\omega$ production are presented and compared with the predictions of the Lund model in order to look for such a suppression. Results on inclusive muoproduction of $\rho^{o}$ mesons in the forward region have been published previously by the EMC [8]. The data presented here significantly extend these earlier results to cover the whole range of Feynman x. The results on $\omega$ leptoproduction rates are the first observation of this inclusive channel.

The data were taken in the M2 muon beam at the CERN SPS using the EMC vertex and forward spectrometers (NA9 experiment). Muons of energy 280 GeV were incident on a 1m long liquid hydrogen target placed in a streamer chamber. Detailed descriptions of the vertex and forward spectrometers are published elsewhere [13,14]. The scattered muon and the fast forward hadrons were detected and momentum analysed in the forward spectrometer. Hadrons of lower momentum and at wider angles were detected in the streamer chamber and vertex spectrometer (the lower cut-off momentum was 200 MeV). Particles were identified in a system of four Cerenkov counters and time of flight hodoscopes. These allowed $\pi$, K and p identification in the laboratory momentum range from 0.5 to 80 GeV. The particle identification system was inefficient for pions with $x_F<-0.2$ and was only used as a consistency check in the $\rho^o$ analysis.

Tracks through the apparatus were reconstructed with an efficiency close to 100% and were passed through a vertex fitting algorithm which assigned them either to the primary vertex or to secondary vertices consistent with particle decays or secondary interactions. Monte Carlo studies show that about 10% of tracks were misassigned to the wrong vertex.

Photons from $\pi^o$ decays were detected in a lead glass calorimeter which was positioned downstream of the forward spectrometer about 19 metres from the centre of the target [15]. It consisted of lead glass blocks, each of thickness 13.6 radiation lengths built in a wall, covering approximately $3m^2$ at the front face. Immediately upstream of the lead glass calorimeter was a lead pre-shower wall of thickness 2.4 radiation lengths. Its purpose was to initiate conversion of photons in order to maximise the energy of the electromagnetic shower deposited in the lead glass. The energy resolution of the calorimeter, averaged over all energies, was approximately 6%. An algorithm was developed to reconstruct $\pi^o$ mesons from the separated or overlapping electromagnetic showers observed in the detector and the width of the $\pi^o$ mass peak was about 40 MeV. The position and geometry of the lead glass calorimeter only allowed the detection of $\pi^o$ mesons with $x_F>0$.

In this paper, standard deep inelastic scattering variables are used. $Q^2$ is the negative four momentum transfer squared, $\nu$ is the laboratory energy of the virtual photon, y is the fraction of the incident beam energy carried by the virtual photon, W is the mass of the hadronic system and the fraction of the proton's momentum carried by the struck quark is given by:

$$x_{Bj} = \frac{Q^2}{2M\nu}$$

where M is the proton mass. The variables W, $Q^2$ and $x_{Bj}$ are related by:

$$W^2 = M^2 + Q^2 \ (1/x_{Bj}-1) \quad .$$

The following variables are commonly used to describe hadron production in lepton-nucleon scattering, $z=E_{lab}/\nu$, where $E_{lab}$ is the laboratory energy of the hadron, $p_T^2$, the transverse momentum squared of the hadron measured with respect to the virtual photon direction and Feynman x is given by $x_F=2p_L^*/W$ where $p_L^*$ is the longitudinal momentum of the hadron in the hadronic centre of mass system.

The data were corrected for the effects of acceptance, identification inefficiency, smearing introduced by the resolution of the apparatus and inefficiencies of the various off-line processes such as vertex fitting and track reconstruction. These corrections were determined by a complete Monte Carlo simulation of the experiment. Deep inelastic scattering events were generated using the Lund String Model [11] for the fragmentation process. Radiative effects due to QED processes and secondary interactions of the produced hadrons in the target material were taken into account. The scattered muon and the secondary hadrons were tracked through the apparatus and the effects of multiple Coulomb scattering were simulated. The detection of photons, from $\pi^o$ decays, in the lead glass was also simulated including the effects of resolution smearing and shower development in the different elements of the detector. These effects were parameterised from measurements

of electron tracks observed in the data [15]. The effects of chamber and hodoscope inefficiencies and smearing were also included and the resulting computed coordinates of the simulated measurements in each detector were passed through the reconstruction programme chain. In this manner the inefficiencies of the apparatus and losses due to imperfections in the off-line analysis were fully corrected for.

## 2. $\rho^0$ Analysis

The data sample consisted of 35624 events of which 25125 passed the following cuts: $Q^2>4$ GeV$^2$, $4<W<20$ GeV, $y<0.85$, $\Theta_\mu>0.75^\circ$, where $\Theta_\mu$ is the angle through which the muon is scattered. These cuts also imply that the laboratory energy of the scattered muon is $E_\mu'>20$ GeV and $\nu<260$ GeV. These criteria were adopted in order to avoid regions where the acceptance was small or varying rapidly and where radiative effects were large. Within these limits $\langle Q^2\rangle=17.5$ GeV$^2$ and $\langle W\rangle=13.3$ GeV.

In order to extract the $\rho^0$ signal all combinations of oppositely charged hadrons were considered ($h^+h^-$) and the pion mass assigned to each. Tracks associated with secondary vertices and identified kaons and protons were excluded. Events with $z_{pair}>0.95$ were also excluded since these contain the elastic contribution. The $h^+h^-$ invariant mass distribution for the entire sample is shown in fig. 1a. The number of $\rho^0$ mesons in this distribution was determined by fitting a relativistic p-wave Breit-Wigner function (BW) and a background function (BG) to the spectrum over the mass range $0.56<m<1.2$ GeV. The fitted function N(m) had the following form:

$$N(m) = a \cdot BW \cdot PS + b \cdot BG,$$

where

$$BG = \exp(-\alpha m) \cdot (1+\beta m + \gamma m^2)$$

and a, b, $\alpha$, $\beta$, $\gamma$ were free parameters. PS is a phase space function, assumed to be of the same shape as the background. The mass and width of the $\rho^0$ were determined from the parameters of the Breit-Wigner function and

were found to be $M_\rho$ =0.768±0.006 GeV and $\Gamma_\rho$ =0.158±0.025 GeV respectively, in excellent agreement with the world average [16]. The smooth curve in fig. 1a represents the fitted background function and fig. 1b shows the mass spectrum after the background has been subtracted.

Due to $\pi^+\pi^-$ combinations arising from $\omega$, $K^o$, $\eta$ and K* decays, where in the latter a K is misidentified as a $\pi$, structures appear in the $h^+h^-$ invariant mass spectrum below 0.5 GeV. As a result of such structures the background distribution is no longer a smooth function of the invariant mass below the $\rho^o$ peak in certain kinematic regions. This causes an uncertainty in the background fit which varies from 15 to 60% depending on the kinematic region, but typically amounted to 30%.

$\rho^o$ production was studied as a function of W, $x_{Bj}$, z, $x_F$ and $p_T^2$ by producing invariant $h^+h^-$ spectra separately for each kinematic region of interest and subtracting the background. The parameters of the $\rho^o$ Breit-Wigner function were fixed during the fitting process at the following values: $M_\rho$=0.769 GeV, $\Gamma_\rho$=0.156 GeV. Both these values were taken from the particle data table [16] and the value of $\Gamma_\rho$ was increased slightly to allow for the effects of the mass resolution of the apparatus. This was measured to be 25 MeV from the observed $K^o$ mass peak [13]. Typical $\chi^2$ per degree of freedom for the fits obtained were in the range 0.8 to 1.5 and the statistical error on the number of $\rho^o$ mesons ranged from 10 to 25%.

Acceptance corrections were calculated for each invariant mass plot using the distributions of generated and processed Monte Carlo events. Since the acceptance corrections for all the kinematic regions mentioned above were only slightly dependent on the invariant mass of the $h^+h^-$ pair in the region of the $\rho^o$ mass, this dependence was ignored during the process of extracting the $\rho^o$ signal. Secondary interactions of the pions from $\rho^o$ decay lead to ~20% of the signal being dispersed into the background and therefore lost after the background subtraction. In order to account for this effect a correction factor was calculated, equal to the ratio of

$\rho^o$ mesons generated and observed in the Monte Carlo events, where the effect of hadron reinteractions were included. The total systematic error was estimated to be ~ 40%. This was obtained by combining the error from the Monte Carlo corrections with that arising from the background subtraction.

The experiment yielded a total number of 7820±600 $\rho^o$ mesons giving an average multiplicity of 0.311±0.024 (stat.) ±0.124 (syst.) $\rho^o$ per event to be compared with the Lund prediction of 0.5 (assuming that the vector/pseudoscalar ratio is one). This discrepancy can be seen as a systematic difference between the Lund prediction and the data points in all the measured distributions.

## 3. ω Analysis

The $\omega \to \pi^o \pi^+ \pi^-$ decay mode (branching ratio 89.9%) has been observed using the $\pi^o$ mesons reconstructed from the lead glass calorimeter in conjunction with data from the charged particle detectors. In order to compensate for the loss of $\pi^o$ mesons due to the low acceptance of the lead glass detector as large a data sample as possible was used. Therefore only two cuts were imposed: $Q^2>2$ GeV$^2$ and $0.05<y<0.9$, leaving a total of 69908 deep inelastic scattering events within these looser cuts. The mean values of the kinematic variables in the data sample were $\langle Q^2 \rangle = 16.3$ GeV$^2$ and $\langle W \rangle = 15.3$ GeV.

To extract the ω signal all combinations of oppositely charged hadrons with a $\pi^o$ were used i.e. $h^+h^-\pi^o$. The significance of the signal and the signal to background ratio were improved by imposing the following requirements on the charged tracks used in the combinations. Only forward charged tracks with $x_F>0$ were considered. This was the most effective cut because the geometry of the lead glass detector restricts full reconstruction of ω mesons to the forward region. Identified protons and tracks without particle identification information were excluded in addition to those with $p_T^2>1$ Gev$^2$. The invariant mass spectrum for the $h^+h^-\pi^o$ combinations after all cuts is shown in fig. 2a. A clear ω signal is seen in two 20 MeV mass bins.

In order to estimate the total number of $\omega$ mesons in the sample two independent methods of background subtraction were attempted. For the first method it was assumed that the $\omega$ signal lay entirely within the two significant bins. The background was approximated by a straight line outside these two bins over the mass range 0.70 to 0.92 GeV. The fitted background was then subtracted leaving the signal as shown in fig. 2b. The Monte Carlo shows that the signal, after background subtraction, should lie over a range of approximately 5 bins and so the resulting number of $\omega$ mesons was corrected by the ratio of $\omega$ mesons lying within the central two bins in the Monte Carlo to the total number in the Monte Carlo peak. The number of $\omega$ mesons obtained in this way was 469±82. As a consistency check a method similar to that described for $\rho$ mesons in the previous section was used to fit the Breit-Wigner and background functions over the mass range between 0.70 to 0.92 GeV. This gave a total yield of 500±96 $\omega$ mesons in good agreement with the first method. These were the yields before acceptance corrections.

The production of $\omega$ mesons was studied as a function of z, $x_F$ and $p_T^2$ by producing invariant mass spectra for each bin of these variables. The straight line fitting method was used to subtract the background for each region and the correction for the losses outside the 2 central mass bins, as explained above, was applied. In order to reduce systematic errors introduced by acceptance corrections only $\omega$'s with $x_F>0.2$ were considered for this part of the analysis. Acceptance corrections were calculated by taking the ratio of $\omega$'s reconstructed in the Monte Carlo to the number generated for each region. The systematic error resulting from the background fit was estimated to be approximately 15%. Once other sources of error due to the Monte Carlo had been taken into account the total systematic error was estimated to be 50%.

## 4. Discussion

The normalised z distribution of the $\rho^o$ production rate is shown in fig. 3. Good agreement with the previous EMC experiment [8] can be seen in the forward region (z>0.3). In the same figure results of two other lepto-

production experiments ($\nu p, \bar{\nu} p$) are plotted [4,10]. All the data seem to be in satisfactory agreement except for the low z region where differences appear. The significantly lower production rate for $0<z<0.3$ observed in the neutrino experiments may be due to the fact that the mean value of the hadronic c.m. energy, W, was much smaller: 4.4 GeV in [4] and 3.7 GeV in [10] as compared to 13.3 GeV for the data presented here. Figure 4 shows the normalised $x_F$ distribution for both the neutrino experiments and the data presented here. The discrepancy observed for $z<0.3$ is also manifest in the region $x_F \sim 0$.

The forward-backward asymmetry (F-B)/(F+B) for $\rho^o$ production is $0.38 \pm 0.06$ (stat.) in agreement with the value of 0.31 predicted by the Lund model.

The average $\rho^o$ multiplicity as a function of $W^2$ and $x_{Bj}$ are shown in figs. 5 and 6, respectively. The shapes of both the $x_{Bj}$ and the W dependences are adequately represented by the model, but as noted above, the model predicts systematically higher yields than observed in the data.

A comparison of the production rates for $\rho^o$ and $\omega$ mesons as functions of z, $x_F$ and $p_T^2$ is shown in figs. 7,8,9 respectively. The production rates of $\rho^o$ and $\omega$ mesons are equal within errors in all three distributions. This result is in reasonable agreement with the predictions of the Lund model. Since both particles have the same valence quarks, effects due to the flavour of the struck quark should not be observed at high z (or $x_F$). This implies that the yeild of $\omega$ and $\rho^o$ should be the same at high z which is consistent with the data.

In conclusion inclusive $\rho^o$ and $\omega$ production rates have been studied in deep inelastic muon scattering on protons. These production rates in the forward direction are found to be equal. This equality implies that there is no suppression of the production of isovector relative to isoscalar mesons in the quark fragmentation process. This is in contrast to the case of the production of vector mesons which is suppressed relative to pseudoscalar mesons. The Lund string model for the fragmentation process gives a reasonable representation of the shape of the data but overestimates the total production rate.

Acknowledgements

We thank all the people in various laboratories who have contributed to the construction, operation and analysis of this experiment. In particular we gratefully acknowledge the support of the CERN staff in operating the SPS, M2 muon beam and computer facilities.

References

[1] R.D. Field and R.P. Feynman, Nucl. Phys. B136 (1978) 1.
[2] I. Cohen et al., Phys. Rev. D25 (1982) 634.
[3] C. del Papa et al., Phys. Rev. Lett. 40 (1978) 90.
[4] P. Allen et al., Nucl. Phys. B194 (1982) 373.
[5] J.P. Berge et al., Phys. Rev. D22 (1980) 1043.
[6] M. Derrick et al., Phys. Lett. 91B (1980) 307.
[7] TASSO, R. Brandelik et al, Phys. Lett. 117B (1982) 135.
[8] EMC, J.J. Aubert et al., Phys. Lett. 133B (1983) 370.
[9] JADE, W. Bartel et al., Phys. Lett. 145B (1984) 441.
[10] H. Grässler et al., CERN/EP 85-41.
[11] B. Andersson, G. Gustafson, Z. Phys. C3 (1980) 223;
T. Sjöstrand, Computer Phys. Comm. 27 (1982) 243.
B. Andersson et al., Phys. Rep. 97 (1983) 31.
G. Ingelman et al., Nucl. Phys. B206 (1982) 239.
[12] B. Andersson, G. Gustafson, LU TP 82-5.
[13] EMC, J. P. Albanese et al., Nucl. Instr. Meth. 212 (1983) 111.
[14] EMC, O.C. Allkofer et al., Nucl. Instr. Meth. 179 (1981) 445.
[15] S. Wheeler, Ph.D. Thesis, University of Sheffield, England (1985).
[16] Particle Data Group, Rev. Mod. Phys. 56 No.2, Part 2 (1986).

Figure Captions

Fig. 1 (a) The $h^+h^-$ invariant mass distribution of the entire sample (after cuts). The curve shows the fit of the background function (BG);
(b) $\rho^o$ peak after background subtraction with the curve of the fitted $\rho^o$ signal.

Fig. 2 (a) The $h^+h^-\pi^o$ invariant mass distribution after cuts (see text);
(b) $\omega$ signal after background subtraction.

Fig. 3 Normalised z distribution of $\rho^o$ ($1/N_\mu \cdot dN_\rho o/dz$) compared with other experiments. The curve shows the prediction of the Lund model.

Fig. 4 Normalised Feynman x distribution of $\rho^o$ compared with other experiments. The curve shows the prediction of the Lund model.

Fig. 5 Average $\rho^o$ multiplicity as a function of the hadronic c.m. energy, W. The curve shows the prediction of the Lund model.

Fig. 6 Average $\rho^o$ multiplicity as a function of $x_{Bj}$. The curve shows the prediction of the Lund model.

Fig. 7 Normalised z distribution of $\omega$ production rate ($1/N_\mu \cdot dN_\omega/dz$) compared with the corresponding $\rho^o$ distribution. The curves show the prediction of the Lund model.

Fig. 8 Normalised Feynman x distribution $\rho^o$ and $\omega$ mesons. The curves show the prediction of the Lund model.

Fig. 9 Normalised transverse momentum $p_T^2$ distribution of $\rho^o$ and $\omega$ mesons compared with other experiments. The curves show the prediction of the Lund model.

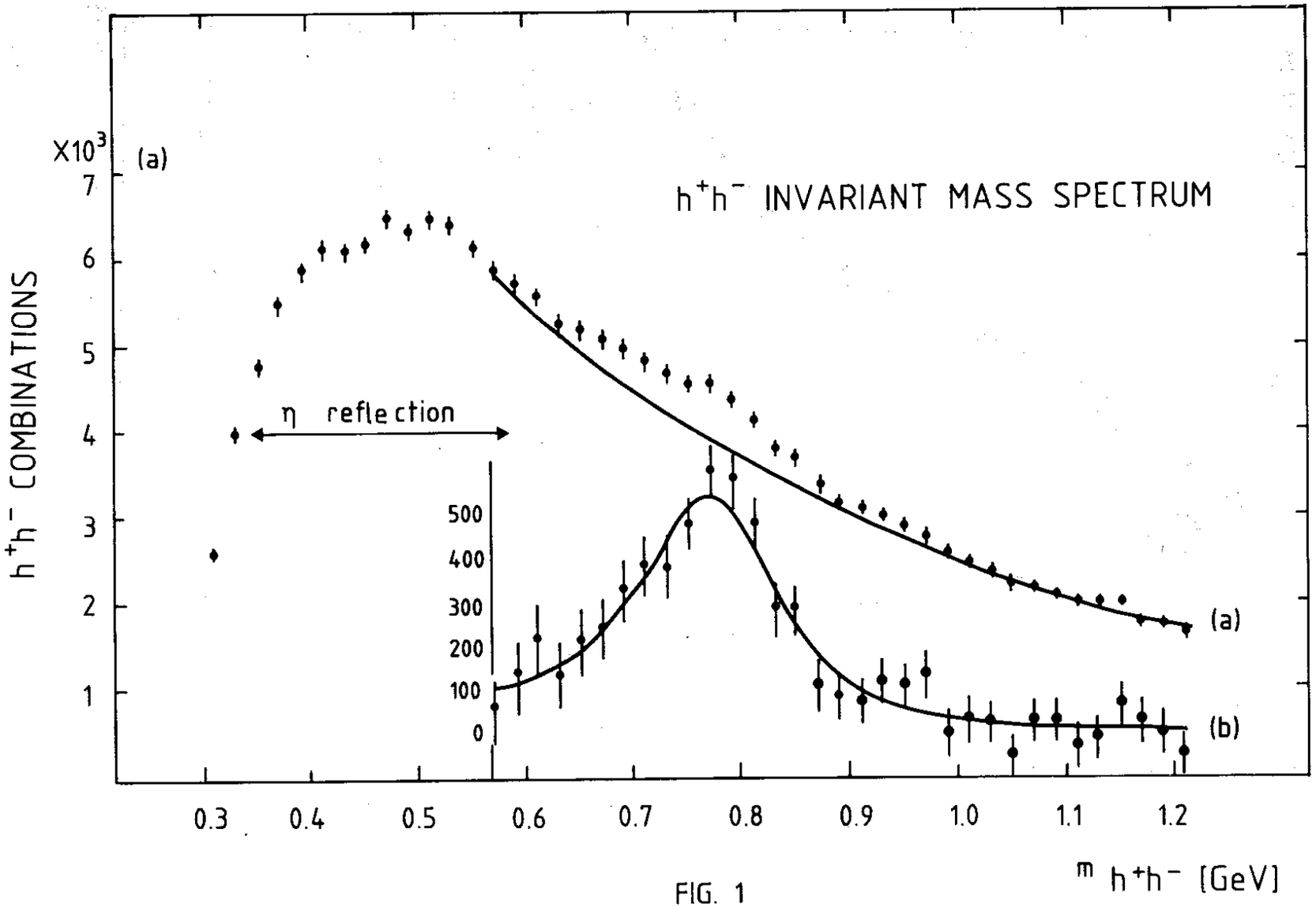
(a)
X10³
h⁺h⁻ INVARIANT MASS SPECTRUM
h⁺h⁻ COMBINATIONS
η reflection
(a)
(b)
m h⁺h⁻ [GeV]

FIG. 1

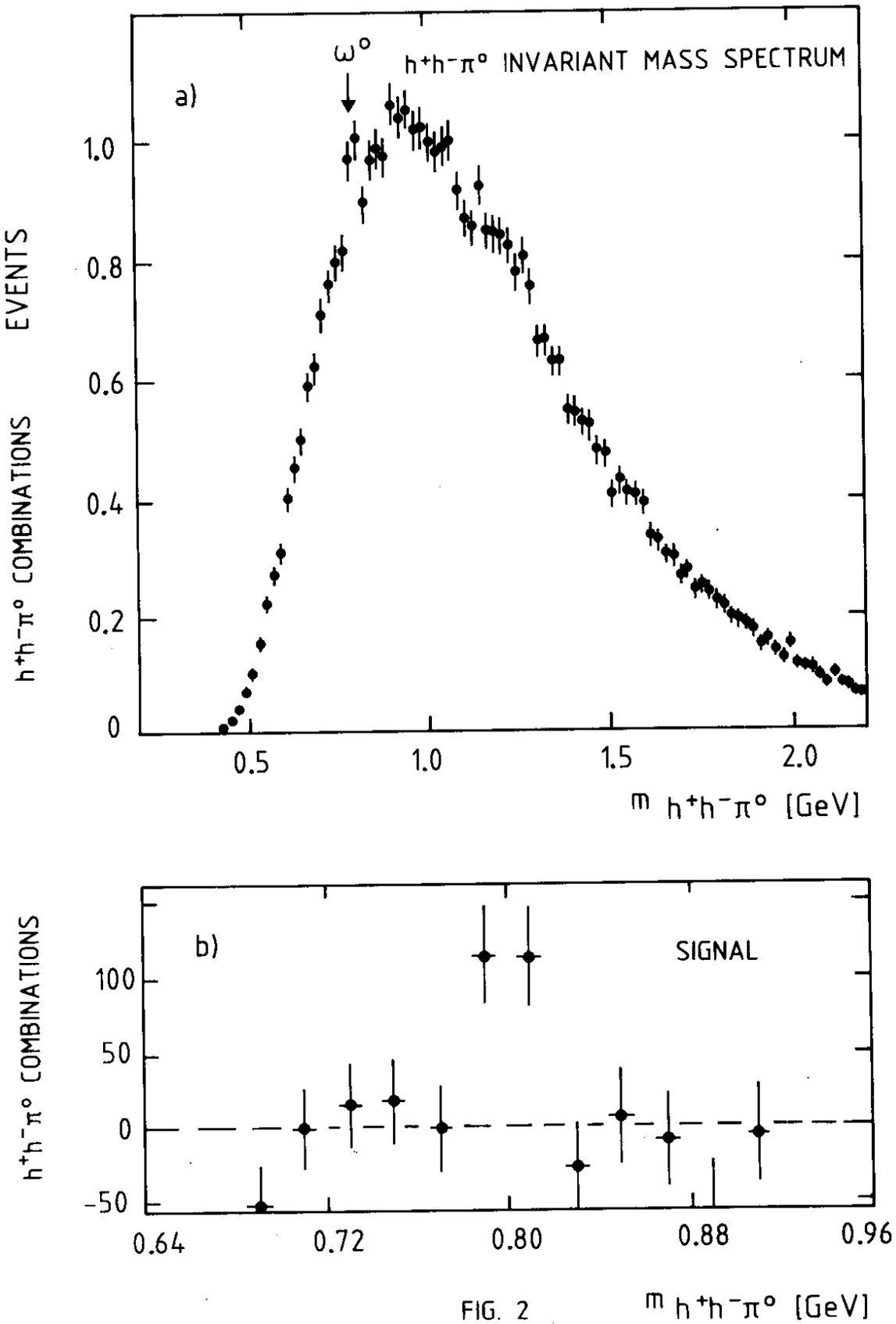
a)
ω°
h⁺h⁻π° INVARIANT MASS SPECTRUM
EVENTS
h⁺h⁻π° COMBINATIONS
1.0
0.8
0.6
0.4
0.2
0
0.5
1.0
1.5
2.0
m h⁺h⁻π° [GeV]
b)
SIGNAL
h⁺h⁻π° COMBINATIONS
100
50
0
-50
0.64
0.72
0.80
0.88
0.96
m h⁺h⁻π° [GeV]

FIG. 2

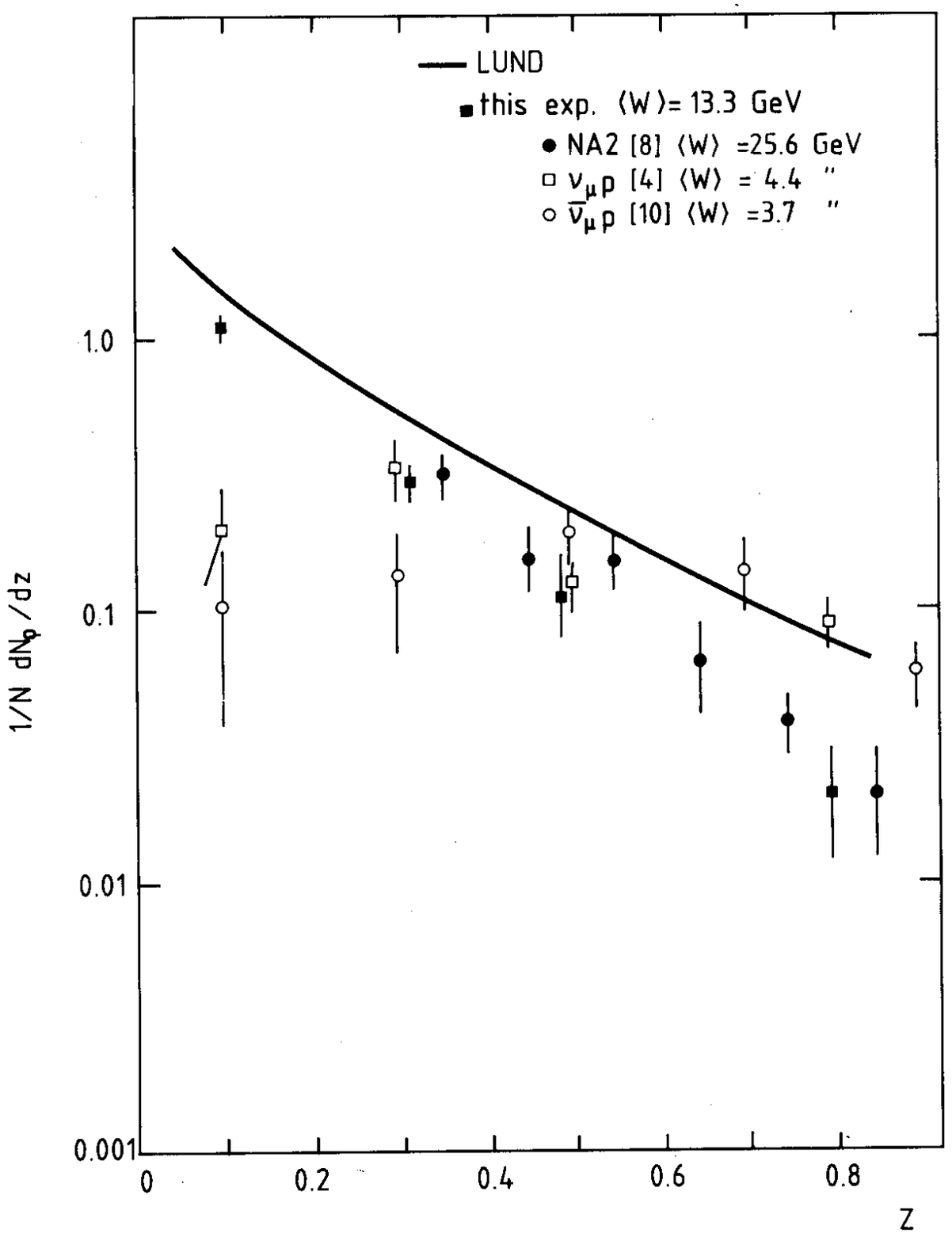
LUND
this exp. ⟨W⟩= 13.3 GeV
NA2 [8] ⟨W⟩ =25.6 GeV
$\nu_\mu p$ [4] ⟨W⟩ = 4.4 "
$\bar{\nu}_\mu p$ [10] ⟨W⟩ =3.7 "
1/N dN$_p$/dz
1.0
0.1
0.01
0.001
0
0.2
0.4
0.6
0.8
Z

FIG. 3

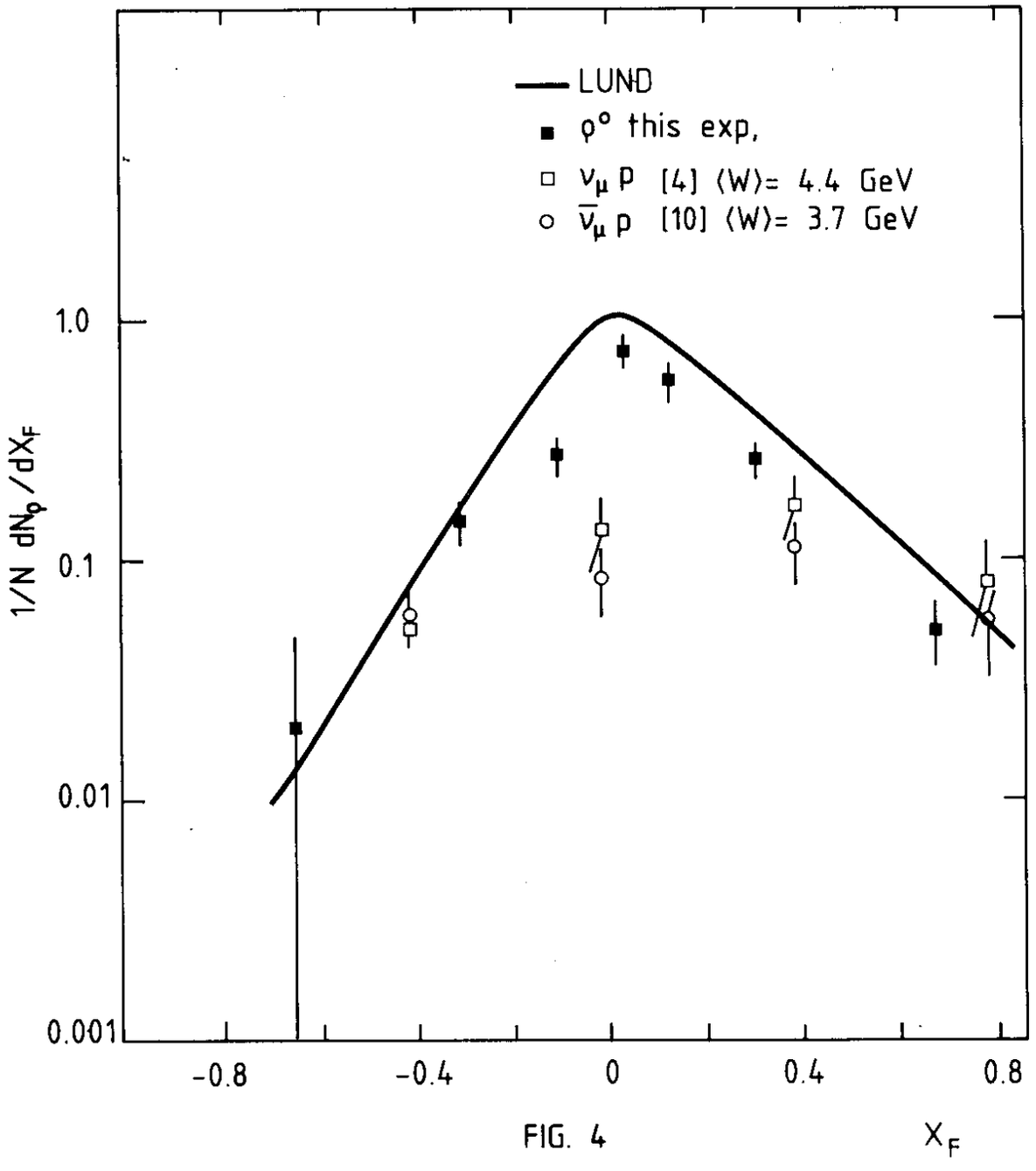
LUND
ρ° this exp,
$\nu_\mu$ p [4] ⟨W⟩= 4.4 GeV
$\bar{\nu}_\mu$ p [10] ⟨W⟩= 3.7 GeV
1.0
0.1
0.01
0.001
1/N dN$_\rho$ /dX$_F$
-0.8
-0.4
0
0.4
0.8
X$_F$

FIG. 4

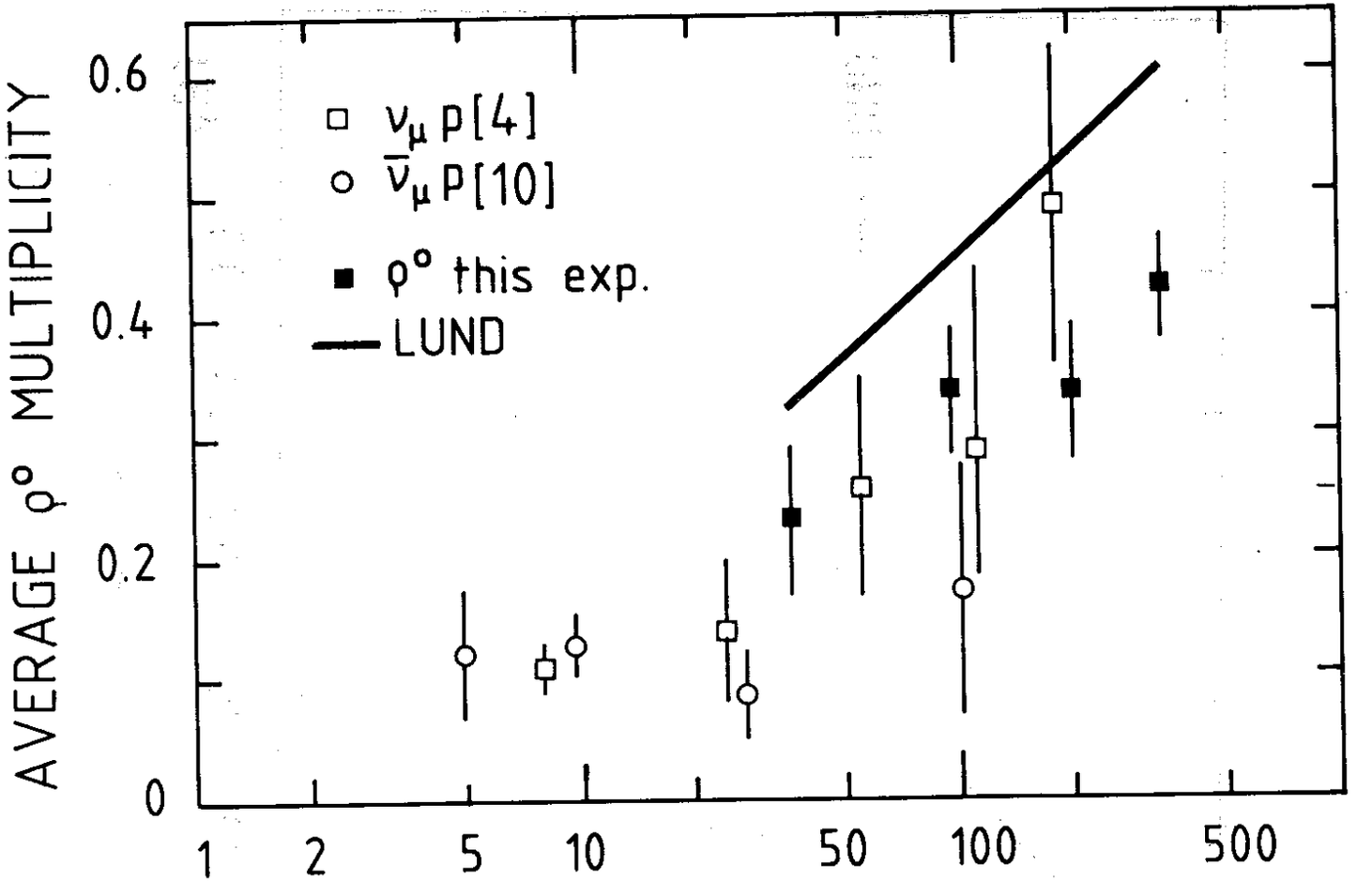
AVERAGE ρ° MULTIPLICITY
0.6
0.4
0.2
0
□ νμ p[4]
○ ν̄μ p[10]
■ ρ° this exp.
— LUND
1
2
5
10
50
100
500
W² [GeV²]

FIG. 5

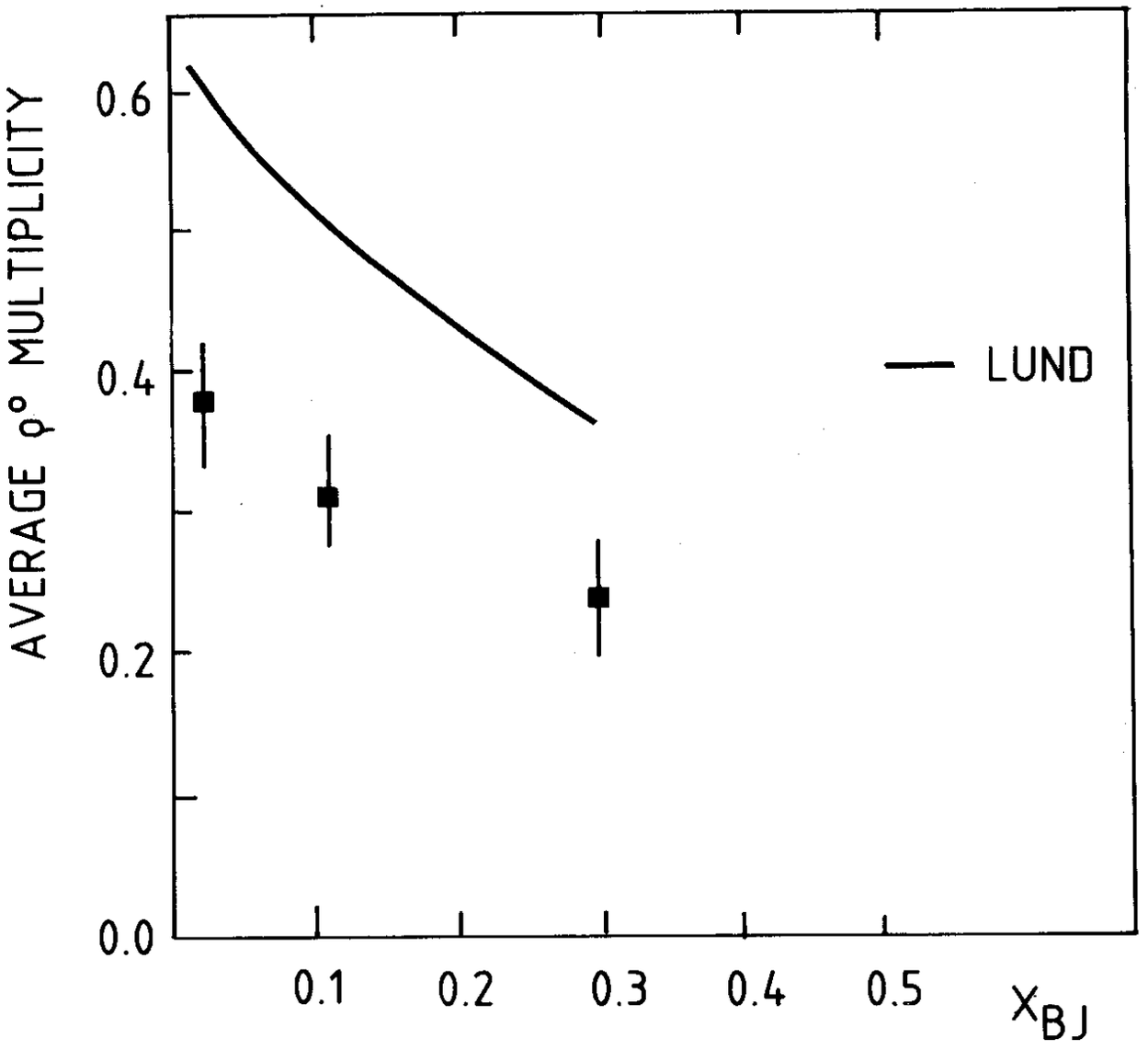


FIG. 6

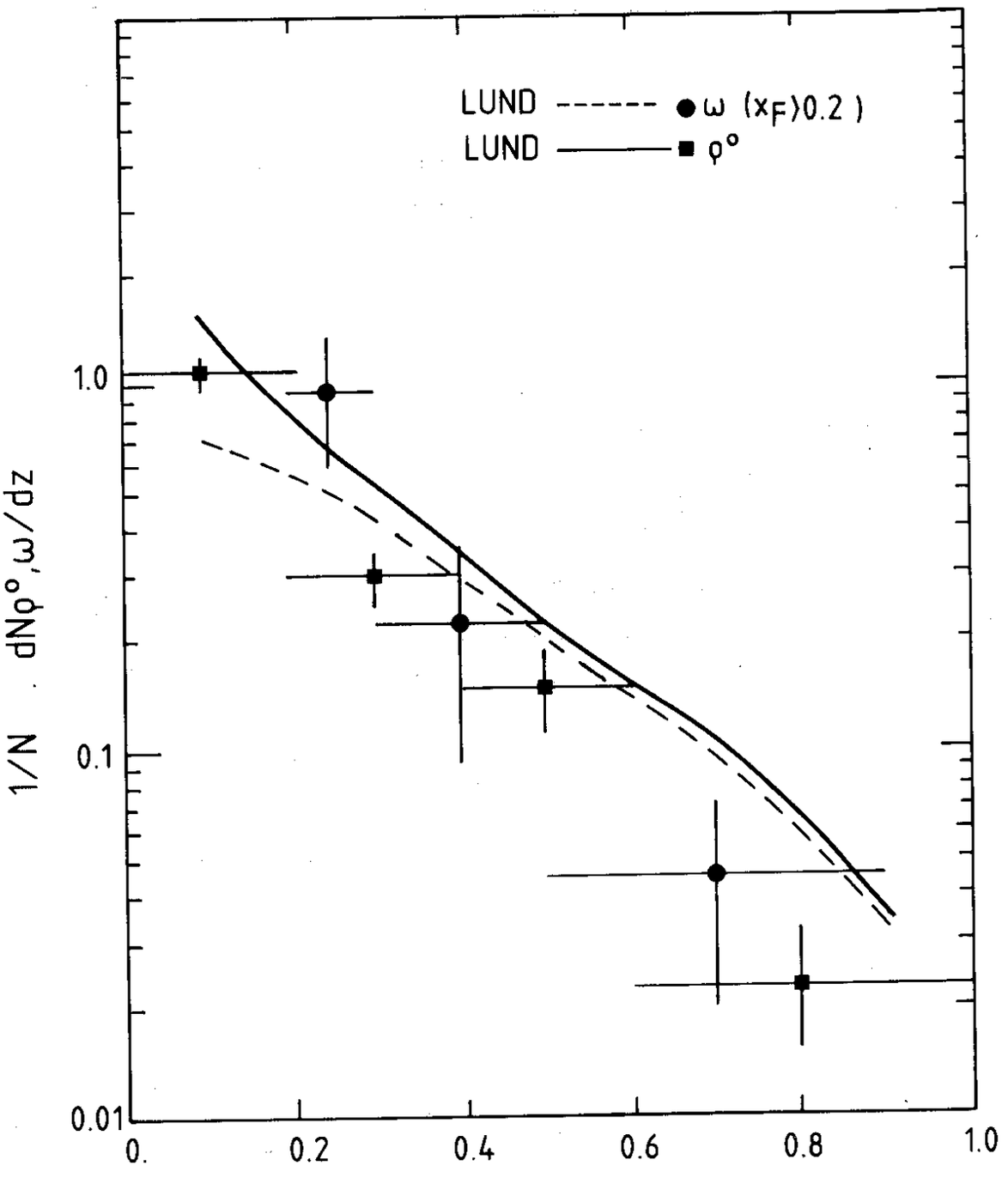


FIG. 7

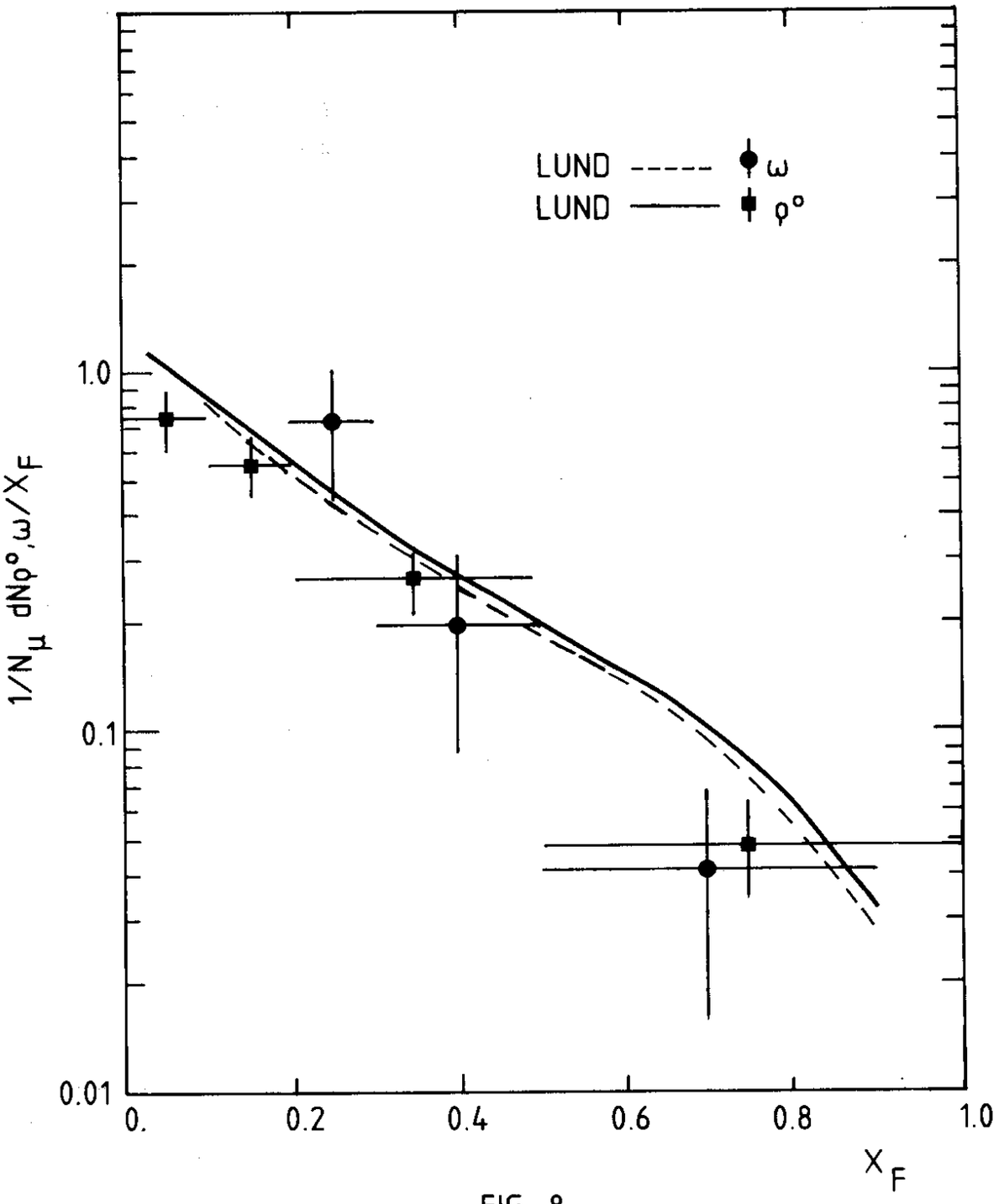
LUND ----- ω
LUND —— ρ°
1.0
0.1
0.01
0.
0.2
0.4
0.6
0.8
1.0
$1/N_\mu \, dN\rho^\circ,\omega/X_F$
$X_F$

FIG. 8

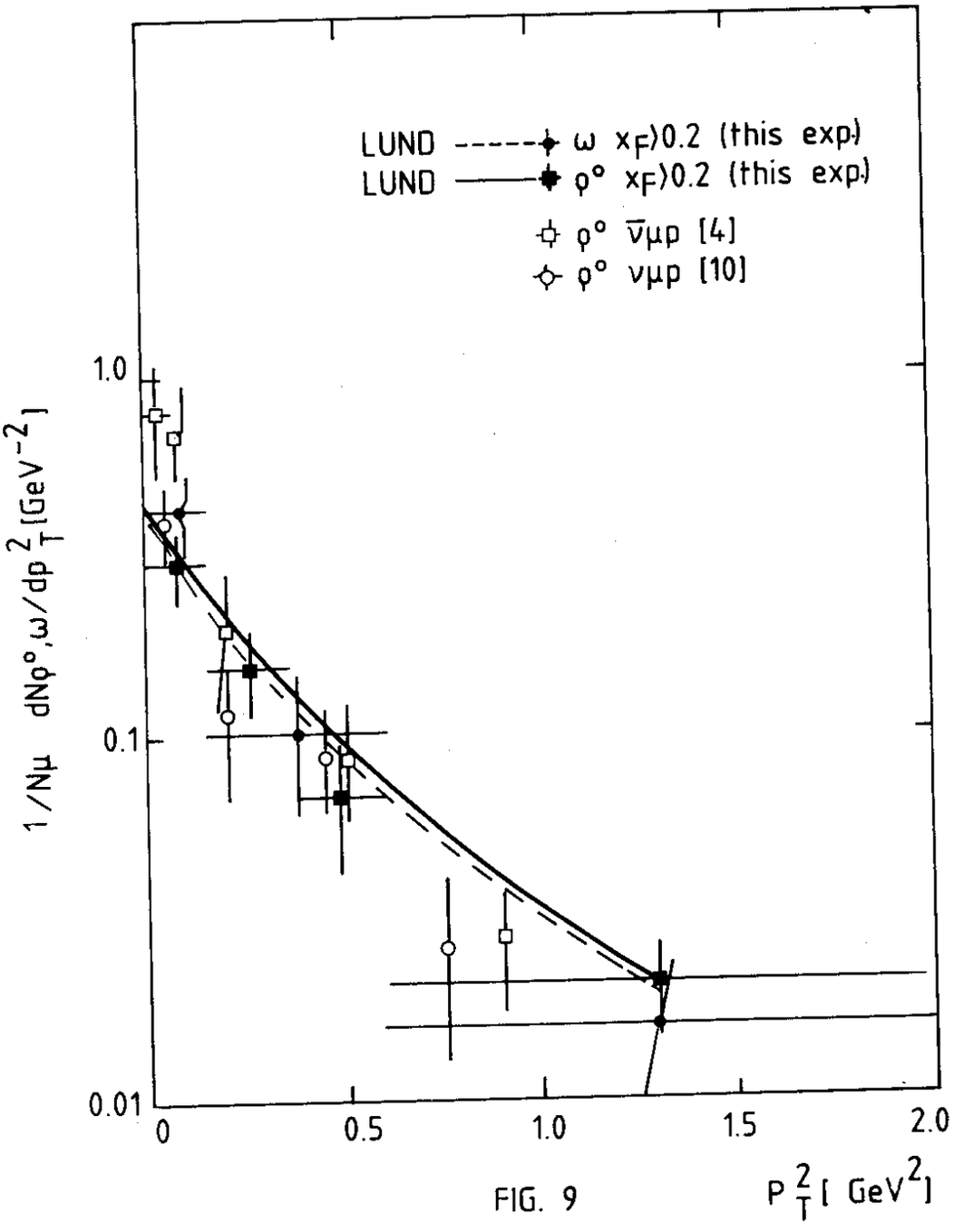
LUND ω $x_F$)0.2 (this exp.)
LUND ρ° $x_F$)0.2 (this exp.)
ρ° $\bar{\nu}\mu p$ [4]
ρ° $\nu\mu p$ [10]
1.0
0.1
0.01
0
0.5
1.0
1.5
2.0
$1/N\mu \; dN\rho^\circ,\omega/dp_T^2 [GeV^{-2}]$
$P_T^2 [GeV^2]$

FIG. 9